YIELD PROCESS OF MILD STEEL IN PLANE PROBLEMS

T. Shioya and T. Machida

Department of Aeronautics, Faculty of Engineering, University of Tokyo, Bunkyo-ku, Tokyo, Japan

Abstract—The analysis of the yield process of mild steel in the plane problems is presented. The continuously distributed dislocations model of the edge component type is adapted with a new application technique as the method of solving the elastic-plane problems. Hahn's equation and the criterion of yield initiation proposed in the previous work [1] are employed as the constitutive relations of mild steel. Examples are taken for the bending of straight beams which is known to accompany the particular patterns with wedge-type plastic-zones. The calculated plastic-zone patterns exhibit close resemblance to the actually observed ones and the scale effect of the patterns given by the analysis is reconfirmed by the related pure bending experiments.

NOTATION

a, n material constants in constitutive equation
C_1', C_2', C_3' material constants in constitutive equation
G shear modulus
h half height of the beam
K, σ_u material constants in the criterion of yield initiation
p normal stress on the surface
r, θ, z cylindrical coordinates
s tangential stress on the surface
x, y, z Cartesian coordinates
α_{hi} dislocation density tensor
$(\beta_p)_{ij}$ plastic distortion tensor
ϵ_{hik} unit permutation tensor
$(\epsilon_p)_{ij}, (\gamma_p)_{ij}$ plastic strain tensor
$\bar{\epsilon}_p$ equivalent plastic strain
$(\dot{\epsilon}_p)_{ij}$ plastic strain rate tensor
κ elastic constant
ν Poisson's ratio
$\partial/\partial v$ differentiation in the direction normal to boundary
σ_{ij} stress tensor
$\bar{\sigma}$ equivalent stress
σ_{ij}' deviatric stress tensor
σ_n, τ_n stress due to unit normal force
σ_t, τ_t stress due to unit tangential force

1. INTRODUCTION

Yielding of mild steel accompanies the plastic-zone pattern of wedge type which is radically different from that expected by the classical theory of plasticity. In the previous paper [1], the elastic–plastic problem was numerically analyzed by the method of continuously distributed dislocations model. The constitutive relations of mild steel were represented by Hahn's equation [2] and the newly proposed criterion for the yield initiation which express the negative slope characteristic in the stress–strain diagram. The numerical examples were taken for twisted round cross-section bars and square ones. The plastic-zone patterns obtained by the calculations were the wedge type similar to the observed ones and had a scale effect arisen from the material nature which is indicated in the criterion of the yield initiation. The corresponding tortional experiments [3] confirmed that the actual yield process is closely simulated by the analysis and that the scale effect expected by the analysis exists also in the actual tortional yielding.

However, the process of the yielding has not been solved other than in the above tortional, or in other words, anti-plane shear cases, in which both the stress and the strain have virtually only one component of the combined shear type. The extension
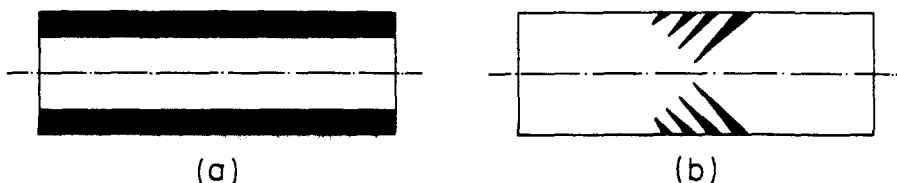
Fig. 1. Plastic-zone patterns in bent straight beams; (a) uniform mode, (b) wedge type mode.

of the problem to the general multi-axial ones can not be done without further advanced knowledge of analyzing the elastic-plastic fields as well as adapting the constitutive relations. In the present paper, an attempt is made for the extension to multi-axial state, especially to the in-plane deformation cases by utilizing new techniques in the method of continuously distributed dislocations model in elastic–plastic problems. The method proposed here can not only be applied to the yield process of mild steel, but also be applied widely to the general elastic–plastic problems. The examples are chosen for the bending of straight beams, because the plastic-zone patterns radically different from that given by the classical plasticity theory have been observed [4], and the knowledge about the scale effect of pattern is expected to be found. Figure 1(a) illustrates the plastic-zone pattern given by the classical plasticity theory and also observed in many other ductile materials, while in Fig. 1(b), the mode which occurs typically in the bending tests of mild steel beam is illustrated. In this paper, the numerical analysis of the yield process is shown for the beams with various heights and further the relating pure bending experiment is exhibited for the comparison with the analysis.

2. ELASTIC-PLASTIC ANALYSIS IN PLANE PROBLEMS

In order to interpret a mechanical phenomenon by analyzing the elastic–plastic continuum problem, the considerations should be taken at two different levels. One is the application of the constitutive relations which represent the mechanical nature of the material in relation to the considered phenomenon, and the other is the means for solving the continuum problem, i.e. the method of determining the stress and strain field in the elastic–plastic body for the applied conditions. Both of them used in the restricted form in the previous work are extended here to apply to the general plane problems.

2.1. Constitutive relations

In the previous work, Hahn's equation and the criterion for the yield initiation were applied as the constitutive relations of mild steel. They appeared in the combined shear form in the actual numerical procedure, however, the generalization of the relations to the multi-axial state were described there by the use of the equivalent stress and the equivalent plastic strain concept [5]. The generalized Hahn's equation is

$$2(\dot{\epsilon}_p)_{ij} = C_1' \left(\frac{\sigma_{ij}'}{\overline{\sigma}/\sqrt{3}}\right) \{C_2' + (\sqrt{3}\overline{\epsilon}_p)^a\}\{\overline{\sigma}/(\sqrt{3}G) - C_3'(\sqrt{3}\overline{\epsilon}_p)\}^n, \tag{1}$$

while the general form of the criterion for the yield initiation is expressed as,

$$\frac{\overline{\sigma}}{\sqrt{3}G} = \frac{\sigma_u}{\sqrt{3}G} - K\sqrt{3}\,\frac{\partial\overline{\epsilon}_p}{\partial v}, \tag{2}$$

where $\partial/\partial v$ means the differentiation in the direction normal to the boundary. As mentioned in the paper, these extensions to the multi-axial state are not universally applicable but are valid in the case when the proportion of the plastic strain components does not change remarkably during the loading. The bending of straight beams is considered to be the case in which this condition is satisfied, so that the eqns (1) and (2) are adapted to the present problem in the next Section.

2.2. Continuously distributed dislocations model

The method of continuously distributed dislocations model is thought to be powerful means for solving the elastic–plastic problems when the boundary condition of the considered body is rather simple. In the previous work, due to the anti-plane problem, the dislocation employed was of the one component screw type with both the dislocation line and the Burgers vector normal to the plane, and the elastic–plane field could be treated without difficulty. However, two problems arise in the case of the plane problem. One is that the deformation involves not only in-plane plastic deformation but also anti-plane plastic deformation and each of them induces couple of edge dislocations. The other is that the stress field of an edge dislocation in a body with boundaries is not given easily even in case of simple boundaries. A method of solving these problems is proposed here.

The density of the continuous distribution of the dislocation α_{hi} is described by the plastic distortion $(\beta_p)_{ij}$ as [6],

$$\alpha_{hi} = -\epsilon_{hlk}(\beta_p)_{kl,l}. \tag{3}$$

In the plane problem, taking the Cartesian coordinates xyz so that the xy-plane becomes the considered plane, the dislocation density tensor has the following edge components given by the plastic strain $(\epsilon_p)_x$, $(\epsilon_p)_y$, $(\gamma_p)_{xy}$ and $(\epsilon_p)_z$, namely,

$$\alpha_{zx} = \frac{\partial}{\partial y}(\epsilon_p)_x - \frac{\partial}{\partial x}(\beta_p)_{yx}, \quad \alpha_{zy} = \frac{\partial}{\partial y}(\beta_p)_{xy} - \frac{\partial}{\partial x}(\epsilon_p)_y, \tag{4}$$

and

$$\alpha_{xz} = -\frac{\partial}{\partial y}(\epsilon_p)_z, \quad \alpha_{yz} = \frac{\partial}{\partial x}(\epsilon_p)_z, \tag{5}$$

where the engineering notation is taken concerning to the shear strain components. It should be noted that the plastic distortion components $(\beta_p)_{yx}$ and $(\beta_p)_{xy}$ in (4) can be arbitrarily taken under the condition that

$$(\beta_p)_{yx} + (\beta_p)_{xy} = (\gamma_p)_{xy}. \tag{6}$$

The stress in the elastic–plastic body comprises the internal stress due to the plastic deformation and the additional stress which satisfies the externally applied conditions. The former can be expressed as the integration of the stress due to each distribution of the dislocations. In the plane problem, the stress due to the plastic deformation can be obtained by superposing the stress due to in-plane plastic deformation $(\epsilon_p)_x$, $(\epsilon_p)_y$ and $(\gamma_p)_{xy}$, and the stress due to anti-plane plastic deformation $(\epsilon_p)_z$. The in-plane plastic deformation can be represented by the edge dislocations with the Burgers vector in the plane, i.e. given by (4). As the stress fields of the unit discrete dislocations are well known, the total stress due to the in-plane plastic deformation in the infinite body becomes

$$\sigma_x(x, y) = \frac{2G}{\pi(\kappa + 1)} \int_{-\infty}^{\infty} \int_{-\infty}^{\infty} [-(y - y')\{3(x - x')^2 + (y - y')^2\}\alpha_{zx}(x', y')$$

$$+ (x - x')\{(x - x')^2 - (y - y')^2\}\alpha_{zy}(x', y')]\{(x - x')^2$$

$$+ (y - y')^2\}^{-2} \, dx' \, dy',$$

$$\sigma_y(x, y) = \frac{2G}{\pi(\kappa + 1)} \int_{-\infty}^{\infty} \int_{-\infty}^{\infty} [(y - y')\{(x - x')^2 - (y - y')^2\}\alpha_{zx}(x', y')$$

$$+ (x - x')\{(x - x')^2 + (y - y')^2\}\alpha_{zy}(x', y')]\{(x - x')^2$$

$$+ (y - y')^2\}^{-2} dx' dy',$$

$$\tau_{xy}(x, y) = \frac{2G}{\pi(\kappa + 1)} \int_{-\infty}^{\infty} \int_{-\infty}^{\infty} [(x - x')\{(x - x')^2 - (y - y')^2\}\alpha_{zx}(x', y')$$

$$+ (y - y')\{(x - x')^2 - (y - y')^2\}\alpha_{zy}(x', y')]\{(x - x')^2$$

$$+ (y - y')^2\}^{-2} dx' dy',$$

$$\begin{cases} \sigma_z(x, y) = \nu\{\sigma_x(x, y) + \sigma_y(x, y)\} & \text{for the plane strain,} \\ \sigma_z(x, y) = 0 & \text{for the plane stress,} \end{cases}$$

(7)

where ν is the Poisson's ratio and $\kappa = 3-4\nu$ for the plane strain or $\kappa = (3 - \nu)/(1 + \nu)$ for the plane stress. On the other hand, the stress field due to the anti-plane plastic deformation $(\epsilon_p)_z$ is evaluated here directly without calculating the stress of each dislocations given in (5). In the case of the plane stress condition, the plastic strain $(\epsilon_p)_z$ exerts evidently no stresses, while, in the case of the plane strain, the stress due to $(\epsilon_p)_z$ is derived as follows. (Although the total strain $\epsilon_z = 0$, the plastic component of the strain $(\epsilon_p)_z$ may exist under the general plane strain condition.) First, the case is considered in which the plastic strain $(\epsilon_p)_z$ is distributed uniformly in the cylinder with the radius r_0 and the axis coincident with the z axis. The stress field in this case is obtained from the strain suppression solution superimposed upon the solution of the internally pressured cylindrical hole to balance the radial stress at $r = r_0$. The solution is

$$\sigma_n = \sigma_\theta = -\frac{G\nu}{1 - \nu} (\epsilon_p)_z, \quad \sigma_z = -\frac{2G}{1 - \nu} (\epsilon_p)_z, \quad \text{for } 0 \leq r < r_0,$$

$$\sigma_n = -\sigma_\theta = -\frac{G\nu}{1 - \nu} \frac{r_0^2}{r^2} (\epsilon_p)_z, \quad \sigma_z = 0, \quad \text{for } r \geq r_0.$$

(8)

By the use of the above equations with the transformation to the xy-coordinates, the stress field due to the distributed plastic strain $(\epsilon_p)_z(x', y')$ in the infinite body is obtained as,

$$\sigma_x(x, y) = -\frac{G\nu}{\pi(1 - \nu)} \int_{-\infty}^{\infty} \int_{-\infty}^{\infty} \frac{(x - x')^2 - (y - y')^2}{\{(x - x')^2 + (y - y')^2\}^2} (\epsilon_p)_z(x', y') dx' dy'$$

$$- \frac{G\nu}{1 - \nu} (\epsilon_p)_z(x, y),$$

$$\sigma_y(x, y) = \frac{G\nu}{\pi(1 - \nu)} \int_{-\infty}^{\infty} \int_{-\infty}^{\infty} \frac{(x - x')^2 - (y - y')^2}{\{(x - x')^2 + (y - y')^2\}^2} (\epsilon_p)_z(x', y') dx' dy'$$

$$- \frac{G\nu}{1 - \nu} (\epsilon_p)_z(x, y),$$

$$\tau_{xy}(x, y) = -\frac{G\nu}{\pi(1 - \nu)} \int_{-\infty}^{\infty} \int_{-\infty}^{\infty} \frac{2(x - x')(y - y')}{\{(x - x')^2 + (y - y')^2\}^2} (\epsilon_p)_z(x', y') dx' dy',$$

$$\sigma_z(x, y) = -\frac{2G}{1 - \nu} (\epsilon_p)_z(x, y).$$

(9)

The sum of the stress fields (7) and (9) is the internal stress due to the plastic deformation in the infinite body under the plane strain condition.

The more practical problem in which the body is not infinitely extended but is contoured by the traction free surface is considered next. In the case of the screw dislocation appeared in the previous paper [1], the stress field in the body with the traction free surface is easily obtained by putting an image dislocation or arrays of image dis-

locations at the appropriate sites. However, this method is not suitable for the case of the edge dislocations, because it is difficult to find a single image dislocation or simple configuration of image dislocations which cancels both the normal and the tangential components of the traction on the supposed free surface. In this case, a practical method may be that instead of cancelling the surface traction due to the individual dislocations, the stress field due to the total plastic deformation is calculated on the assumption of infinite body first, and the elastic solution cancelling the traction on the surface is superimposed upon it. As the elastic solution to satisfy the surface condition, techniques of solving usual elastic problems may be utilized. For example, in the case of a straight beam with the height $2h$ (the beam lies between $y = \pm h$), the problem turns to finding the elastic solution of the beam, the upper and the lower surfaces of which are subjected by the stress distribution induced by the plastic deformation. This becomes essentially the solution of an integral equation, since the analytical solution of the stress field in a semi-infinite elastic body ($y \leqq h$) subjected by a concentrated force at a point $x = 0, y = h$ on the surface is known as [7]

$$
\left.
\begin{aligned}
(\sigma_n)_x(x, y) &= \frac{2}{\pi} \frac{x^2(y - h)}{\{x^2 + (y - h)^2\}^2}, \\[2mm]
(\sigma_n)_y(x, y) &= \frac{2}{\pi} \frac{(y - h)^3}{\{x^2 + (y - h)^2\}^2}, \\[2mm]
(\tau_n)_{xy}(x, y) &= \frac{2}{\pi} \frac{x(y - h)^2}{\{x^2 + (y - h)^2\}^2},
\end{aligned}
\right\} \tag{10}
$$

for the unit normal force and

$$
\left.
\begin{aligned}
(\sigma_t)_x(x, y) &= \frac{2}{\pi} \frac{x^3}{\{x^2 + (y - h)^2\}^2}, \\[2mm]
(\sigma_t)_y(x, y) &= \frac{2}{\pi} \frac{x(y - h)^2}{\{x^2 + (y - h)^2\}^2}, \\[2mm]
(\tau_t)_{xy}(x, y) &= \frac{2}{\pi} \frac{x^2(y - h)}{\{x^2 + (y - h)^2\}^2},
\end{aligned}
\right\} \tag{11}
$$

for the unit tangential force, respectively. The solution of the integral equation is easily obtained by the following iterative procedure. First, the initial stress on the upper surface is calculated on the assumption of the infinite body and it is denoted by $p_0(x)$ and $s_0(x)$ for the normal and the tangential components, respectively. Next, the complementary stress cancelling the above stress is superimposed on the upper surface and the resultant stress at the lower surface is calculated which is denoted by $p_1(x)$ and $s_1(x)$, for the normal and the tangential components, respectively. This procedure is repeated alternatively on either the upper or the lower surface, i.e. the stress components superimposed on the upper surface are

$$
\left.
\begin{aligned}
p_{2n}(x) &= \int_{-\infty}^{\infty} p_{2n-1}(x')(\sigma_n)_y(x - x', -h)\, dx' \\[2mm]
&\quad - \int_{-\infty}^{\infty} s_{2n-1}(x')(\sigma_t)_y(x - x', -h)\, dx', \\[2mm]
s_{2n}(x) &= - \int_{-\infty}^{\infty} p_{2n-1}(x')(\tau_n)_{xy}(x - x', -h)\, dx' \\[2mm]
&\quad + \int_{-\infty}^{\infty} s_{2n-1}(x')(\tau_t)_{xy}(x - x', -h)\, dx',
\end{aligned}
\right\} \tag{12}
$$

and on the lower surface, the superimposed stress components are

$$
\left.
\begin{aligned}
p_{2n+1}(x) &= \int_{-\infty}^{\infty} p_{2n}(x')(\sigma_n)_y(x - x', -h)\, dx' \\
&\quad + \int_{-\infty}^{\infty} s_{2n}(x')(\sigma_t)_y(x - x', -h)\, dx', \\
s_{2n+1}(x) &= \int_{-\infty}^{\infty} p_{2n}(x')(\tau_n)_{xy}(x - x', -h)\, dx' \\
&\quad + \int_{-\infty}^{\infty} s_{2n}(x')(\tau_t)_{xy}(x - x', -h)\, dx'.
\end{aligned}
\right\}
\qquad (13)
$$

Usually the solution of this procedure is considered to converge rapidly.

3. NUMERICAL ANALYSIS OF THE YIELD PROCESS IN BENT BEAMS

By the use of the constitutive relations and the method of continuously distributed dislocations model in the plane problem proposed in the previous Section, the numerical calculations for the yield process of the bent straight beams were carried out. The calculation procedure is similar to that of the tortional problems of the previous work, namely, according to the description form of Hahn's constitutive equation, the problem is treated as an initial valued problem of the first order differential equation. The stress field for the known plastic strain field in the beam is calculated through the method of continuously distributed dislocations model. For the given stress and strain field, the criterion of the yield initiation is examined in the unyielded region and the plastic strain increment is calculated by Hahn's constitutive equation. It is assumed that the condition of the plane strain is satisfied and that the pure bending load is applied in the manner of linearly increasing moment. In the numerical calculations, the beam section is divided into square elements, the sides of which are parallel or normal to the beam surface.

Although the plastic strain patterns actually appear are such as illustrated in Fig. 1(b), the uniform mode shown in Fig. 1(a) should be at least one of the theoretical solutions. The reason it does not occur is considered that the non-uniform patterns existing as small irregularities in the material develop during the yield process owing to the nature of the constitutive relations. Therefore, some kind of non-uniformity should be introduced also in the numerical calculation to represent this effect. In the present work, the criterion of the yield initiation is assumed to be satisfied on the beginning of loading at a pair of symmetrical elements on the upper and the lower surfaces of the beam. Further, in order to introduce the non-symmetricity with respect to the vertical axis connecting the above elements, the plastic strain initiation is assumed

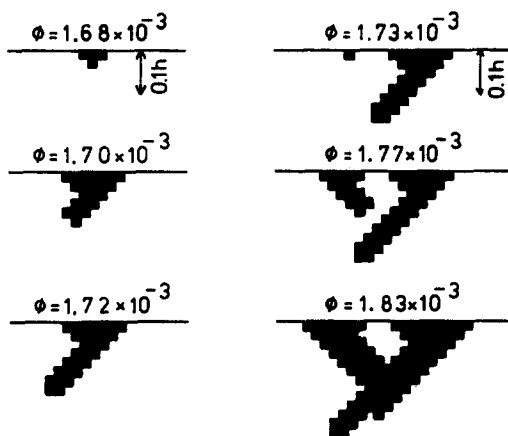
Fig. 2. Calculated growth process of plastic-zone in the yielding of a bent straight beam (plane strain analysis); $K/h = 3.33 \times 10^{-4}$, $\dot{\phi} = 10^{-4}s^{-1}$.
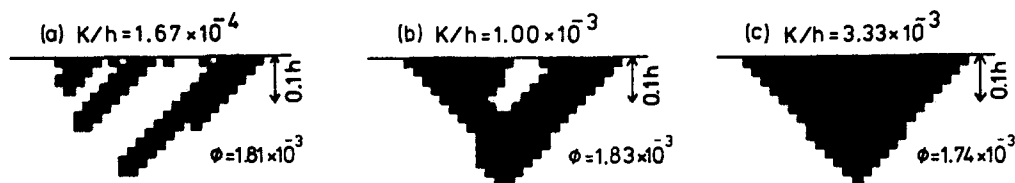
Fig. 3. Effect of K/h on the calculated plastic-zone pattern in the yielding of a bent straight beam (plane strain analysis); $\phi = 10^{-4}s^{-1}$; (a) parallel mode, (b) opposing mode, (c) symmetrical mode.

to precede on one side elements at the first time when the criterion becomes satisifed on both side elements in the process of the spreading of the initial plastic zone. Besides these treatment, no special contrivance is added further.

In the numerical calculations, the same values as in the previous work were given to the material constants in the constitutive relations (1) and (2), namely, $C_1' = 10^{98}s^{-1}$, $C_2' = 10^{-4}$, $C_3' = 1.1 \times 10^{-2}$, $a = 1.5$, $n = 35$ and $\sigma_u/G = 3.9 \times 10^{-3}$. Besides, $\nu = 0.3$ was added here. The manner of taking the time step interval in the calculation was also the same as in the previous work. An example of the calculated growth process of the plastic-zone in the plane strain analysis is shown in Fig. 2. Since the plastic-zone pattern is symmetrical with respect to the neutral axis, only the upper side of the beam section is viewed in the figure. The loading rate was chosen as $\phi = 10^{-4}s^{-1}$, where ϕ is the tensile strain on the upper surface at the infinite ends of the beam. The non-dimensional parameter K/h was taken as 3.33×10^{-4}, where h is the half height of the beam. Figure 3 shows the plastic-zone patterns for $K/h = 1.67 \times 10^{-4}$, 1.0×10^{-3} and 3.33×10^{-3}. In the case of the twisted round bars calculated in the previous work, the scale effect in the plastic-zone patterns appeared in the manner that the number of plastic-zone wedges increases and the wedges become sharper as the diameter of the bar increases. However, the calculated plastic-zone patterns in Fig. 3 shows that in the case of the bent beams, the patterns are classified into three modes according to the beam heights. When the beam is high, the plastic-zone wedge which appears first in the beam develops sharply along the direction of maximum shear, i.e. 45° to the beam line, and the subsequent wedges develop in parallel to the first wedge (parallel mode), while in the middle height beam, although the first wedge develops similar to that of the high beam, the development of the second wedge is towards the first wedge (opposing mode). On the other hand, in the low height beam, a wide plastic-zone wedge almost symmetrical with respect to the vertical axis develops without producing subsequent separate plastic-zone (symmetrical mode).

4. EXPERIMENT

As stated before, it has already been known since the earlier time that the bending of mild steel beams accompanies a particular plastic-zone pattern like that shown in Fig. 1(b). However, whether the scale effect obtained by the theoretical analysis of the previous Section would actually exist or not has not been examined experimentally nor been paid attention to. In order to certify this effect, four point bending tests changing the size of the specimen were carried out. The chemical composition of the mild steel used in the experiment is listed in Table 1. The height of the specimen beam was varied from 3 to 25 mm, while the width of the beam was kept the constant value of 15 mm. Figure 4 shows the example of the plastic-zone patterns of the bent specimens visualized as the strain figures obtained by the Fry's etching method. From the figure, it is seen that the plastic-zone pattern of the high beam is of the parallel mode type, and as the height becomes lower, the pattern transits to the opposing mode as expected by the theoretical analysis. However, the transition from the opposing mode to the symmetrical one in the lower beam region is not sufficiently clear in the experiment on account of the obscure strain figure in the small specimens. The fact that the higher

Table 1. Chemical composition of specimen materials used in bending experiment. (wt %)

C	Si	Mn	P	S	Cu	Ni	Cr	Al	Fe
0.01	0.01	0.32	0.14	0.11	0.02	0.03	0.01	0.009	bal

the beam, the sharper the plastic-zone becomes is the same tendency as in the calculated results.

5. DISCUSSIONS AND CONCLUSIONS

The method of analyzing the yield process of mild steel in the plane problem was established by extending the method of continuously distributed dislocations model and the constitutive relations to the multi-axial state. The yield process of the bending

(a)

(b)

(c)

Fig. 4. Effect of the beam height on the plastic-zone pattern in the yielding of a bent straight beam visualized as the strain figures; (a) $2h = 25$ mm, (b) $2h = 10$ mm, (c) $2h = 3$mm.

of straight beams was analyzed as the numerical example of the plane problem and the calculated plastic-zone patterns are closely similar to the actual ones. The method presented here can be applied widely to the general elastic–plastic plane problems.

Concerning to the scale effect in the bending problem, the change in the mode of the plastic-zone patterns may be qualitatively explained in terms of the applied stress gradient in the normal direction to the beam surface. The stress at the inner region in the high beam is closer to the stress on the surface than in the case of the lower beam so that the region is more easily affected by the plastic strain on the surface and as the results, the sharp wedge patterns may develop inwards, while in the lower beam, the stress on the surface is relatively superior to that of the inner region so that the plastic region is apt to widen along the surface. This explanation may directly apply to the transition from the opposing mode to the symmetrical mode as well as the sharpening tendency of the wedges with the beam height. The transition from the parallel to the opposing mode is interpreted in a more complex manner. The total plastic displacement in the wedge region which is defined as the integration of the plastic strain in the region decreases more gradually along the wedge in the high beam than in the low beam, which may also be explained by the above discussion. Due to the stress rearrangement by this gradual decrease of the plastic displacement in the wedge, the position at which the second plastic-zone wedge starts in the high beam becomes more apart from the first wedge in relation to the wedge size. This effect on the second starting position is seen in the numerical analysis of the present work. It is thought that the direction of the maximum stress gradient at the second starting position transits from the inner direction (i.e. towards the first wedge) to the outer direction as the starting position becomes apart.

The quantitative comparison between the result of the numerical analysis and that of the experiment does not seem satisfactory concerning to the scale effect even though the difference of the material is in consideration. If the value of K is taken as in the previous work [1], the calculated plastic-zone patterns of Fig. 3(a)–(c) correspond to the cases of $h = 432.0$ mm, 72.0 mm and 21.6 mm, respectively, which are fairly larger than those of the bending experiment (Fig. 4). However, the experiment of the twisted round bars has given a smaller value of K from the comparison with the calculated plastic-zone patterns [3], and if the latter value is used, the cases of Fig. 3 correspond to $h = 90$ mm, 15.0 mm and 4.5 mm, which are less different from those of the experiment. This fact suggests that the constants in the criterion of the yield initiation is rather sensitive to the material and the estimation of the values by the experiment is fairly influenced by the test conditions.

The numerical analyses of the present work and the previous work do not cover all the types of loading, however, it can be stated that some kind of scale effect is necessarily involved in the yield process of mild steel under any type of loading, since the criterion of the yield initiation includes a constant which is related with the dimension of length.

REFERENCES

1. T. Shioya and J. Shioiri, Elastic–plastic analysis of the yield process in mild steel. *J. Mech. Phys. Solids* **24**, 187–204 (1976).
2. G. T. Hahn, A model for yielding with special reference to the yield point phenomena of iron and related bcc metals. *Acta Met.* **10**, 727–738 (1962).
3. T. Shioya, T. Machida, R. Ishida and Y. Fujiura, Scale effect of the plastic zone pattern in the yield process of mild steel. *Proc. 22nd Japan Congr. Material Res.* 47–50 (1979).
4. F. Nakanishi, Strength of mild steel beams under uniform bending. *J. Japan Soc. Mech. Engrs* **32**, 171–178 (1929).
5. R. Hill, *The Mathematical Theory of Plasticity*, Chap. II. Oxford University Press (1950).
6. T. Mura, Continuous distribution of moving dislocations. *Phil. Mag.* **8**, 843–857 (1963).
7. S. Timoshenko and J. N. Goodier, *Theory of Elasticity*, 2nd Edn, p. 275. McGraw-Hill, New York (1951).